



# Metformin prevents liver tumourigenesis by attenuating fibrosis in a transgenic mouse model of hepatocellular carcinoma

Ram C. Shankaraiah<sup>1</sup> · Elisa Callegari<sup>1</sup> · Paola Guerriero<sup>1</sup> · Alessandro Rimessi<sup>1</sup> · Paolo Pinton<sup>1</sup> · Laura Gramantieri<sup>2</sup> · Enrico M. Silini<sup>3</sup> · Silvia Sabbioni<sup>4</sup> · Massimo Negrini<sup>1</sup>

Received: 2 April 2019 / Revised: 27 May 2019 / Accepted: 30 May 2019  
© The Author(s), under exclusive licence to Springer Nature Limited 2019

## Abstract

Metformin is a hypoglycaemic agent used to treat type 2 diabetes mellitus (DM2) patients, with a broad safety profile. Since previous epidemiological studies had shown that the incidence of hepatocellular carcinoma (HCC) decreased significantly in metformin treated DM2 patients, we hypothesised that intervention with metformin could reduce the risk of neoplastic transformation of hepatocytes. HCC is the most common primary liver malignancy and it generally originates in a background of liver fibrosis and cirrhosis. In the present study, we took advantage of a transgenic mouse (TG221) characterized by microRNA-221 overexpression, with cirrhotic liver background induced by chronic administration of carbon tetrachloride (CCl<sub>4</sub>). This mouse model develops fibrosis, cirrhosis and liver tumours that become visible in 100% of mice at 5–6 months of age. Our results demonstrated that metformin intervention improves liver function, inhibits hepatic stellate cell (HSC) activation, reduces liver fibrosis, depletes lipid accumulation in hepatocytes, halts progression to decompensated cirrhosis and abrogates development HCC in CCl<sub>4</sub> challenged transgenic mouse model. The study establishes the rationale for investigating metformin in cirrhotic patients regardless of concomitant DM2 status.

## Introduction

Liver cancer is the second leading cause of cancer related death worldwide, with about 841,000 new cases annually [1]. Therapeutic options are limited, and prognosis is generally poor, with curative approaches available only for early stages of disease. Hepatocellular carcinoma (HCC) arises from hepatocytes and is the most common primary

liver cancer. About 80 to 90% of all HCCs occurs within a background of chronic liver disease and cirrhosis, which represents the most important risk factor for HCC [2]. The extended time of progression from liver fibrosis to malignancy make individuals at risk for HCC identifiable and candidates for chemoprevention strategies to delay or stop the natural course of chronic liver disease and curtail HCC incidence and mortality [3].

Hepatitis B vaccination programs or anti-hepatitis C therapeutics are examples of approaches that not only protect from viral infection, but also reduce the incidence of virus-associated HCC [4, 5]. However, non-viral causes namely alcoholic or non-alcoholic fatty liver disease (NAFLD) and non-alcoholic steatohepatitis (NASH) account for nearly 46% liver cancer deaths [6]. Additionally, increasing epidemic of obesity and type 2 diabetes mellitus (DM2), both important risk factors of NAFLD and NASH, might emerge as dominant risk factors for HCC incidence in future [7, 8]. Hence, prevention programs can have an important impact in decreasing HCC occurrence.

Metformin is a first-line dimethylbiguanide hypoglycaemic agent used to treat DM2 patients, with a broad safety profile. Abundant epidemiological data have indicated that incidence of several cancers, including HCC decreased

**Supplementary information** The online version of this article (<https://doi.org/10.1038/s41388-019-0942-z>) contains supplementary material, which is available to authorized users.

✉ Massimo Negrini  
ngm@unife.it

<sup>1</sup> Department of Morphology Surgery and Experimental Medicine, University of Ferrara, Ferrara, Italy

<sup>2</sup> Center for Applied Biomedical Research, St. Orsola-Malpighi University Hospital, 40138 Bologna, Italy

<sup>3</sup> Section of Anatomy and Pathology, University Hospital of Parma, Parma, Italy

<sup>4</sup> Department of Life Sciences and Biotechnology, University of Ferrara, Ferrara, Italy

significantly in DM2 patients on metformin treatment compared to dietary restrictions alone, insulin or sulfonylureas [9–12]. Several mechanisms have been proposed for metformin action. They include metabolic reprogramming of cancer cells by activation of 5' adenosine monophosphate-activated protein kinase (AMPK) [13, 14], altering vascular and immune tumour microenvironment [15, 16] and suppressing stemness of cancer cells [17, 18].

We hypothesized that intervention with metformin in non-diabetic liver fibrosis/cirrhosis setting could reduce tumour formation. Despite numerous pharmacoepidemiological data on cancer preventive effects of metformin in DM2, impact of metformin on HCC prevention in non-diabetic liver disease is largely unexplored. A meta-analysis of anti-tumour effects of metformin in HCC animal models concluded that pre-clinical studies lacked sufficient indication of stage at which metformin use is beneficial [19]. This is at least in part due to a dearth for animal models that uniformly manifest HCC with a background of cirrhosis, typically seen in human disease. In the present study, hepatoprotective effect of metformin was investigated in transgenic mice that develop liver tumours in a cirrhotic liver background.

## Materials and methods

### CCI4 induced HCC mouse model with cirrhosis background and metformin intervention

Male miR-221 transgenic (TG221) strain with B6D2F2 background mice (4–6 weeks of age) were administered 150  $\mu$ l of olive oil (Arm 1) or 20% v/v CCI4 in olive oil (Arm 2) by oral gavage (p.o.) three times a week for a duration of 14 weeks. Metformin intervention (Arm 3) was started after 3 weeks of initiating CCI4 challenge at 300 mg/kg body weight (BW) daily p.o., dissolved in distilled water. Dosage of metformin used in present study was calculated using Reagan-Shaw method [20]. Briefly mouse equivalent dose (mg/kg) = human dose (mg/kg)  $\times$  human ( $k_m$ )/mouse ( $k_m$ ). Where  $k_m$  factor, unique to each species is a constant used to normalize dosage based on body surface area. For a 60 kg human adult  $k_m$  equates to 37 and a 20 g mouse  $k_m$  equals 3. Metformin daily dosage in humans range from 1000 mg to 2500 mg, usually prescribed twice daily. Therefore, a dose of 1500 mg per day in human adults translated to approximately 300 mg/kg per day mouse dosage [15]. Mice were randomly assigned to the different experimental arms. Ellipsoid volume of surface nodules were measured ex-vivo as  $V = (\pi/6) \times (\text{long axis}) \times (\text{short axis})$  [9, 21]. Mice were maintained in vented cabinets at 24 °C with a 12-h light-dark cycle. Food and water were provided ad libitum. All animal procedures were performed

according to the guidelines of the Italian Ministry of Health Public Health Service Policy on Care and Use of laboratory animals, and in accordance with a protocol approved by the Institutional Animal Care Committee of University of Ferrara and Italian Ministry of Health.

### Transaminase assays

At time points of 0, 3, 6, 9, 14 weeks blood sampling of 20  $\mu$ l was done by tail vein nick and post 24 weeks by cardiac puncture after mice were euthanized by isoflurane inhalation anaesthesia and subsequent cervical dislocation. Serum was collected from blood samples of corresponding experimental groups and AST and ALT levels assayed with respective colorimetric kits (Sigma; MAK055/MAK052) according to manufacturer's instructions and absorbance read on Tecan Infinite F200 Pro plate reader (TECAN, Switzerland).

### Ultrasonography

Liver ultrasonography (Philips iU22 with a linear transducer) surveillance was performed at fortnightly intervals after 14 weeks to monitor growth of liver nodules. Mice were anesthetized with intraperitoneal (i.p.) cocktail of ketamine (90 mg/kg BW) and xylazine (9 mg/kg BW) in 0.9% sodium chloride solution and were always placed on temperature-controlled heating pads during the entire imaging procedure. DICOM files were analyzed using an open source medical image viewer (Horos project v3.1.2).

### Cell lines and reagents

Human HCC cell line HepG2 (ATCC HB-8065, Rockville, MD, USA and authenticated by the provider by cytogenetic analysis) were cultured as monolayers in IMDM media (Sigma; I6529) supplemented with 10% fetal bovine serum (FBS, Sigma; F7524), 0.1% gentamicin (Gibco; 15750-037). Human hepatics stellate cell line LX-2 (generous gift from Vienna Hepatic Experimental Hemodynamic-HEPEX Lab at the Medical University of Vienna) were cultured as monolayer in DMEM media (Sigma; D5796) supplemented with 5% FBS, 0.1% gentamicin. All cell lines were maintained in a 37 °C humidified incubator containing 5% CO<sub>2</sub> and tested free of mycoplasma contamination (MycoAlert Mycoplasma Detection kit, cat#LT07-418, Lonza). Metformin (Sigma; D150959) was dissolved in phosphate-buffered saline (PBS) at a concentration of 1 mol/L, stored at –20 °C and subsequently diluted to appropriate concentrations in complete media without antibiotics for each assay. All cell culture experiments were carried out within eight passages after being thawed, performed in triplicates and repeated twice.

## 147 Western blot

148 Snap frozen tissues were homogenized in RIPA buffer  
 149 (Sigma R0278) with protease/phosphatase inhibitors (com-  
 150 plete ULTRA/PhosSTOP tablets, Roche) and sodium  
 151 orthovanadate using a tissue homogenizer. Lysates were  
 152 centrifuged at 14,000 rpm for 20 min at 4 °C. Protein con-  
 153 centration of the supernatant was measured by modified  
 154 Lowry protein assay before boiling in 4× Laemmli buffer.  
 155 Approximately 10 µg of protein from lysates were loaded on  
 156 precast PAGE, separated by electrophoresis and transferred  
 157 to pvdf membranes with Trans-Blot Turbo system (Bio-  
 158 Rad). Non-specific binding was blocked by 5% non-fat milk  
 159 for 1 h. Membranes were incubated overnight at 4 °C with  
 160 primary antibodies. Primary antibodies used: LKB1  
 161 (Cat#3047), AMPKα (Cat#2532), pAMPKα Thr-172  
 162 (Cat#2535), AKT (Cat#4691), pACC Ser-79 (Cat#3661),  
 163 ACC (Cat#3662), S6 (Cat#2217), p4E-BP1 (cat#2855), 4E-  
 164 BP1 (Cat#9644), PARP (Cat#9542), cleaved-PARP  
 165 (Cat#9544) at 1:1000 dilution and pAKT Ser473  
 166 (Cat#4060), pS6 Ser-235/236 (Cat#4858) at 1:2000 dilu-  
 167 tion. All antibodies listed above were obtained from Cell  
 168 Signalling Technologies (Danvers, MA, USA). Other anti-  
 169 bodies used were: α-SMA (1:500 Cat#A5228, Sigma) and  
 170 GAPDH as loading control (1:5000 Cat# TA890003, Ori-  
 171 gene). Following day, after a brief wash, membranes were  
 172 incubated with anti-rabbit HRP (Cell Signaling 1:1000) or  
 173 anti-mouse HRP (Cell Signaling 1:5000) secondary anti-  
 174 bodies. Membranes were developed with Clarity western  
 175 ECL (Bio-Rad) or high-sensitivity Westar Supernova  
 176 Blotting Substrate (Cyanagen, Italy) and chemilumines-  
 177 cence visualized on Chemidoc XRS+ imaging system (Bio-  
 178 Rad).

## 179 Histology and immunocytochemistry

180 Formalin-fixed paraffin embedded (FFPE) samples were  
 181 sectioned into 5 µm-thick sections and stained with  
 182 hematoxylin-eosin (H&E) and Masson's trichrome accord-  
 183 ing to standard procedures. All slides were reviewed by the  
 184 same pathologist. Formalin-fixed samples were further  
 185 processed with 30% sucrose and embedded in optimal  
 186 cutting temperature (OCT) compound and frozen to -80 °  
 187 C. OCT embedded samples were sectioned into 10 µm-thick  
 188 sections and stained with Oil Red O (ORO) staining  
 189 according to standard procedures. Lipid droplets were  
 190 morphometrically quantified on ORO stained sections with  
 191 image processing software (ImageJ, NIH) as described  
 192 previously [22, 23]. In total, 10 fields of visions were  
 193 analyzed for each section and lipid droplet size and number  
 194 were averaged for comparison. HepG2 cells cultured with  
 195 or without metformin were stained with ORO and images  
 196 were captured. Amount of lipid droplets were quantified

semi-quantitatively by extracting ORO from cells in 100%  
 propanol and absorbance measured at OD450nm with  
 Tecan Infinite F200 Pro plate reader (TECAN, Switzer-  
 land). Fixed LX-2 cells cultured on polylysine coated round  
 coverslips were incubated with α-SMA antibody (1:100,  
 Cat#A5228, Sigma), followed by incubation with Alex  
 Fluor® 488 goat-anti mouse (1:1000, Cat#A11001, Thermo  
 Fischer scientific) for 1 h at room temperature. Cells were  
 then mounted with Vectashield mounting medium with  
 DAPI, observed with a Nikon Eclipse TE2000-E confocal  
 microscope (Nikon, Florence, Italy) and images acquired by  
 Nikon DXM1200F digital camera.

## Gene expression microarray analysis

Gene expression profiling was done with an Agilent whole  
 mouse gene expression 8 × 60 K microarray (Cat# G4852A,  
 Agilent Technologies). One-colour microarray-based gene  
 expression was analyzed according to standard operating  
 procedures from Agilent Technologies. Briefly, total RNA  
 from snap frozen samples was extracted using Trizol  
 Reagent (FS-881, FMB, Treviso, USA) according to  
 manufacturer's instructions. Quantity and quality of RNA  
 was assessed with RNA-600 nanochip (Agilent Technolo-  
 gies) on Agilent 2100 Bioanalyzer. Samples with RNA  
 integrity number above 8 were utilized for microarray. Total  
 RNA of 100 ng from each sample was used to synthesize  
 cyanine 3-CTP (Perkin-Elmer Life Sciences, Boston, USA)  
 labelled cRNA with Low RNA Input Linear Amplification  
 kit (Agilent Technologies). Labelled RNA was hybridized  
 at 65 °C for 17 h at 10 rpm in an incubator. Images of slides  
 were captured by the Agilent scanner and raw microarray  
 data was obtained by accompanying Agilent Feature  
 Extraction Software (v10.5). Quantile normalization of raw  
 microarray expression and downstream analysis was per-  
 formed with Qlucore omics explorer (v3.4, Qlucore AB,  
 Sweden). Differentially expressed genes in two group  
 comparison were sorted based on analysis of variance, *F*-  
 test and <0.01 false discovery rate (FDR-q). Heat maps  
 were generated based on hierarchical clustering of samples  
 and genes. Genes that were differentially expressed with  
 fold change >1.5 and FDR <0.01 between two groups  
 (CCl4+metformin vs CCl4 livers) on an unpaired t-test  
 were considered for Gene Set Enrichment Analysis  
 (GSEA). Differentially expressed genes were summarized  
 into mouse Entrez gene IDs and mapped to human ortho-  
 logs using mapping reports from Mouse Genome Infor-  
 matics database (Jackson laboratories- [www.informatics.jax.org](http://www.informatics.jax.org)). Differential genes between phenotypes were ranked  
 according to t-statistics. Metformin mediated up-regulated  
 genes were given a positive score and corresponding down-  
 regulated genes a negative score compared to CCl4 only  
 livers. Pre-ranked GSEA was applied with GSEA

248 3.0 software [24, 25]. The curated canonical pathways from  
 249 MSigDB (Molecular Signature Database - Hallmark,  
 250 KEGG and Reactome) were used. Statistical significance of  
 251 normalized enrichment score was estimated using  
 252 phenotype-based permutation (1000) testing and FDR  
 253 <0.25. Raw data from microarrays are available at Gene  
 254 Expression Omnibus (GEO accession number:  
 255 GSE131175). Predicted miR-221 mouse gene targets were  
 256 retrieved from miRDB excluding targets with >70 predic-  
 257 tion score (244 genes, Supplementary excel file) and com-  
 258 monality was compared with metformin mediated  
 259 dysregulated proteins elucidated by immunoblotting [26].

## 260 Statistical analyses

261 In mouse studies, no animals were excluded from the ana-  
 262 lysis. Investigators were not blinded after simple randomi-  
 263 zation method used to assign mice to different experimental  
 264 arms. Sample size for animal experiments were calculated  
 265 to be seven mice for each CCl4 and metformin + CCl4  
 266 groups at significance level alpha of 5%, a priori power  
 267 80% and estimated effect size (*d*) 1.5, using G\*Power  
 268 software [27]. An unpaired *t* test (two-tailed with unequal  
 269 variance) was used to compare differences between two  
 270 groups throughout the study and significance with a  
 271 threshold of *P*-value <0.05 was considered. Variances  
 272 between groups were compared by *F*-test. Summary data  
 273 are expressed as mean ± standard deviation (SD). Statistical  
 274 analysis was performed using data analysis software Prism  
 275 6.0 (GraphPad Software Inc., La Jolla, CA, USA).

## 276 Results

### 277 CCl4 induced cirrhosis and HCC in the TG221 mouse 278 model

279 We utilized a previously established transgenic mouse strain  
 280 (TG221), which is predisposed to the development of liver  
 281 tumours [28]. Recurrent liver injury was induced in 4 to  
 282 6 weeks old male mice by oral gavage of 150 µl 20% CCl4  
 283 v/v in olive oil, three times a week for the duration of  
 284 14 weeks. Control TG221 mice were administered 150 µl of  
 285 olive oil only, at the same time points (Fig. 1a). Serum  
 286 levels of liver enzymes aspartate transaminase (AST) and  
 287 alanine transaminase (ALT) significantly increased with  
 288 time, denoting liver damage in CCl4 challenged mice when  
 289 compared to olive oil treated mice (Fig. 1b). Notably, serum  
 290 transaminase levels remained high also after discontinuation  
 291 of CCl4, thus indicating that an irreversible stage of liver  
 292 damage was reached.

293 Mice were sacrificed 3, 6, 9 and 14 weeks after initiating  
 294 CCl4 or olive oil gavage (*n* = 2 for each time point) and

295 liver tissues were harvested. Macroscopically, livers 295  
 296 showed signs of the CCl4-induced damage, characterized 296  
 297 by a yellowish pale appearance rather than dark red, a 297  
 298 harder than normal consistency, an irregular surface with 298  
 299 nodules of different sizes (Fig. 1c). Trichrome staining 299  
 300 revealed a sequential progression of liver fibrosis with 300  
 301 sustained CCl4 challenge. Thin septal fibrosis was evident 301  
 302 at 3 weeks, progressing to bridging fibrosis by 6 and 302  
 303 9 weeks but still maintaining liver architecture. However, 303  
 304 14 weeks of CCl4 challenge led to progression of fibrosis, 304  
 305 distortion of liver architecture, nodule formation and ascites 305  
 306 typical of cirrhosis (Fig. 1d, Supplementary Fig. 1a).

307 Following cessation of Olive oil (Arm1, *n* = 7) or CCl4 307  
 308 gavage (Arm2, *n* = 7), mice were monitored by abdominal 308  
 309 ultrasonography (USG) at bi-weekly intervals for signs of 309  
 310 tumour development. While small liver nodules could be 310  
 311 identified at week 14, frank liver masses were detected by 311  
 312 USG at 24 weeks only in Arm2 mice (Supplementary 312  
 313 Fig. 1a, b).

314 At the experimental end-point (24 weeks), explorative 314  
 315 laparotomy revealed hepatomegaly and multiple surface 315  
 316 nodules in 100% of CCl4 challenged mice. Olive oil treated 316  
 317 mice did not present with hepatomegaly or surface nodules 317  
 318 in the liver (Supplementary Fig. 1c, d). Histological 318  
 319 assessment of livers and corresponding nodules revealed 319  
 320 different phases of tumorigenesis from dysplastic focal 320  
 321 nodular hyperplasia (FNH)-like, to frank HCC with abun- 321  
 322 dant steatosis (Supplementary Table 1). In accordance with 322  
 323 gross pathology, histopathology of livers from olive oil 323  
 324 treated mice did not reveal any evident liver lesions. 324

### 325 Metformin intervention abrogates fibrosis and 326 steatosis in CCl4 challenged TG221 mice

327 In patients, progression from asymptomatic liver fibrosis to 327  
 328 decompensated cirrhosis takes years. Furthermore, once 328  
 329 end-stage liver disease is reached, liver transplantation 329  
 330 represents the only option to improve quality of life in these 330  
 331 patients [29]. Therefore, implementation of early interven- 331  
 332 tion strategies are aimed at preventing deterioration of 332  
 333 fibrotic disease [30, 31]. Since, in the TG221 mouse model, 333  
 334 CCl4 induced fibrosis as early as 3 weeks, we hypothesized 334  
 335 that chemoprevention strategies at this stage could possibly 335  
 336 prevent the progression of disease. TG221 mice (*n* = 7) 336  
 337 were treated daily by oral gavage with metformin at a 337  
 338 dosage of 300 mg/kg, starting at 3 weeks post induction of 338  
 339 CCl4-challenge (Fig. 2a). Dosage of metformin used in 339  
 340 present study was calculated according to the Reagan-Shaw 340  
 341 method [20] to approximate human daily dosage of 341  
 342 1500 mg, typically taken by patients affected by type 2 DM. 342  
 343 These mice were administered CCl4 up to 14 weeks, like in 343  
 344 Arm2 control, and daily metformin treatment was continued 344  
 345 until the experimental end-point at 24 weeks. Of note, 345



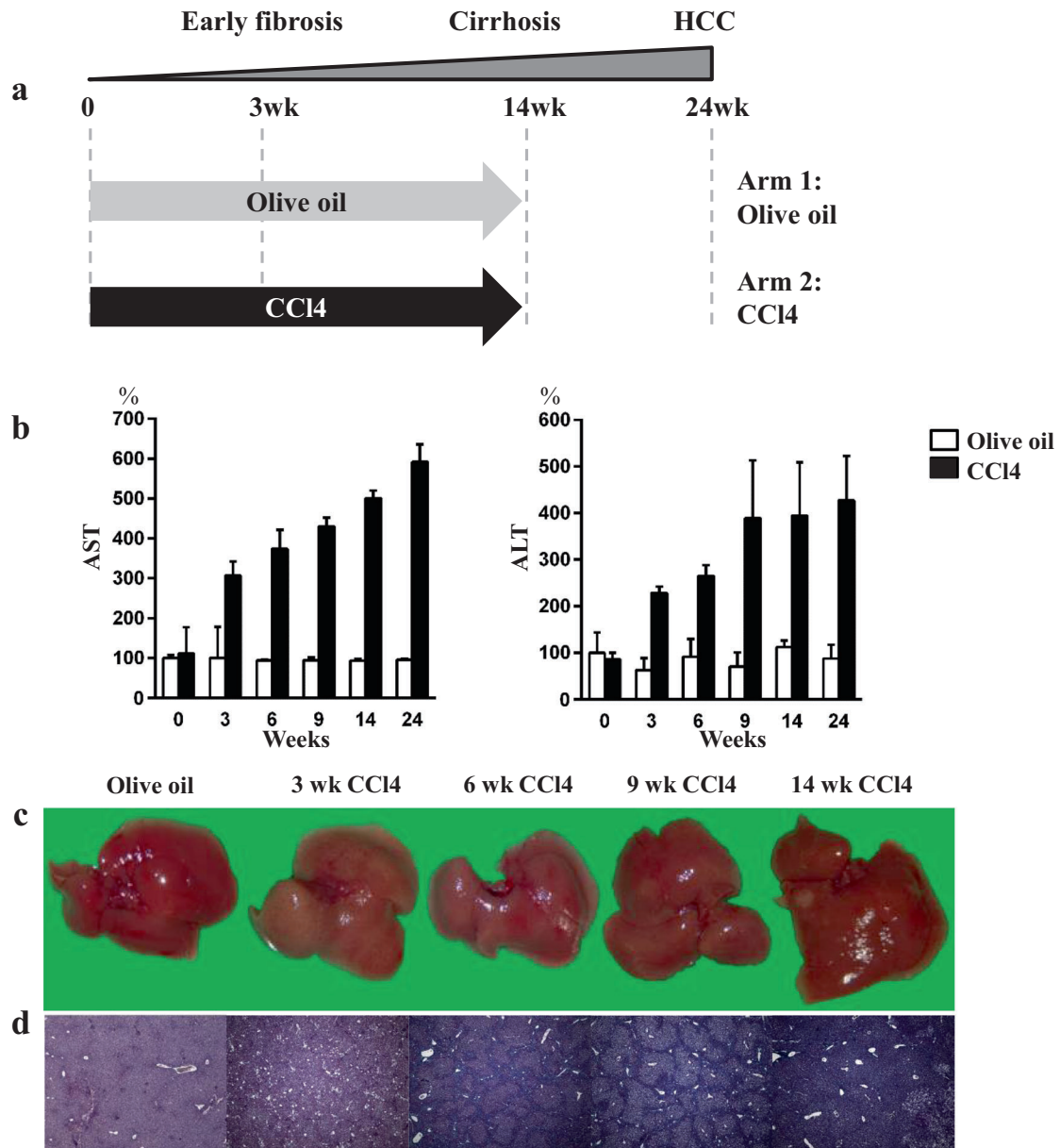


**Fig. 1** CCl4 administration induces chronic liver damage and fibrosis in the liver of mice. **a** Experimental design: 4 to 6 weeks old mice were administered olive oil (Arm1) or 20% CCl4 in olive oil (Arm2) per os (p.o.) for 14 weeks. Experimental end-point was at 24 weeks after initiation of CCL4 challenge. **b** Liver damage was detected by the increase of liver Aspartate transaminase (AST) and Alanine

transaminase (ALT) enzyme levels. AST-ALT levels are depicted as percentage change between Olive oil and CCl4 experimental arms. **c** Images of mouse livers at the indicated time of sacrifice. **d** Trichrome staining of FFPE livers at corresponding same time points and treatments as of (c) (x40 magnification)

346 treatment with metformin significantly reduced serum levels  
347 of AST and ALT (Fig. 2b). Three-hours post final metformin  
348 gavage, mice were sacrificed, and livers collected.

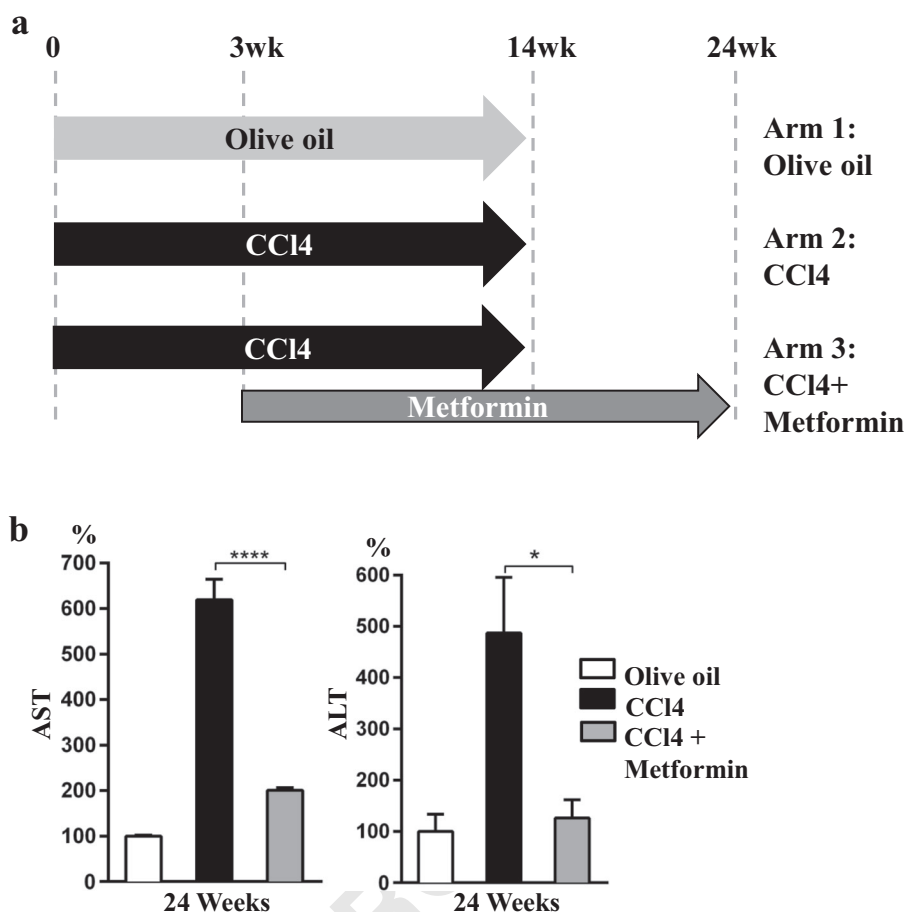
349 Metformin intervention significantly decreased CCl4  
350 induced liver fibrosis as evidenced by collagen content,  
351 immunoblotting for  $\alpha$ -SMA and gene expression analysis  
352 (Fig. 3a–c). The reduction of *Coll1a1*, *Col3a1*, *Col4a1*  
353 expression and  $\alpha$ -SMA protein levels in livers indicates an  
354 inhibitory effect on hepatic stellate cells (HSCs) activation

355 by metformin. We confirmed that metformin abrogated the  
356 expression of  $\alpha$ -SMA in the human HSCs LX-2 cells  
357 in vitro (Supplementary Fig. 2a, b).

358 Microvesicular steatosis is another feature of cirrhosis  
359 where excess lipid droplets are observed in hepatocytes  
360 [32, 33]. Metformin significantly decreased accumulation of  
361 lipid droplets in livers when compared to untreated CCl4  
362 challenged mice (Fig. 4a, b). One of the well-studied  
363 mechanism of actions of metformin is its ability to activate

**Fig. 2** Experimental design of metformin treatments. **a** Mice were administered olive oil (Arm1) or 20% CCl<sub>4</sub> in olive oil (Arm2 and Arm3) per os (p.o.) for 14 weeks. Additionally, mice in Arm3 were treated with Metformin at 300 mg/kg dosage p.o., starting at 3 weeks post initiation of CCl<sub>4</sub> challenge, until experimental end point at 24 weeks. ( $n = 7$  in each experimental arms).

**b** Metformin intervention improved serum levels of the liver enzymes AST and ALT. \*\*\*\* $P < 0.0001$  \* $P < 0.05$ . AST-ALT levels are depicted as percentage change between experimental arms at 24 weeks time-point



364 AMPK [34]. AMPK has been attributed to be a master  
 365 regulator of cellular metabolism and energy homeostasis  
 366 [35, 36]. Here, we confirmed by immunoblotting, that  
 367 metformin increased the levels of total LKB1 leading to  
 368 increased phosphorylation of AMPK at Thr-172. As a  
 369 consequence of activation of AMPK, downstream inhibi-  
 370 tory phosphorylation of ACC at Ser-79 was also uncovered  
 371 (Fig. 4c). The enzyme ACC catalyzes the carboxylation of  
 372 acetyl-CoA to malonyl-CoA, the rate-limiting step in fatty  
 373 acid synthesis [37]. Abrogation of ACC activity might  
 374 account for metformin mediated reduction of de novo  
 375 lipogenesis in hepatocytes. Further, in vitro metformin  
 376 significantly reduced intracellular lipid droplets in HepG2  
 377 cells in a dose and time dependent manner (Supplementary  
 378 Fig. 3).

### 379 Metformin intervention prevents HCC in CCl<sub>4</sub> 380 challenged TG221 mice

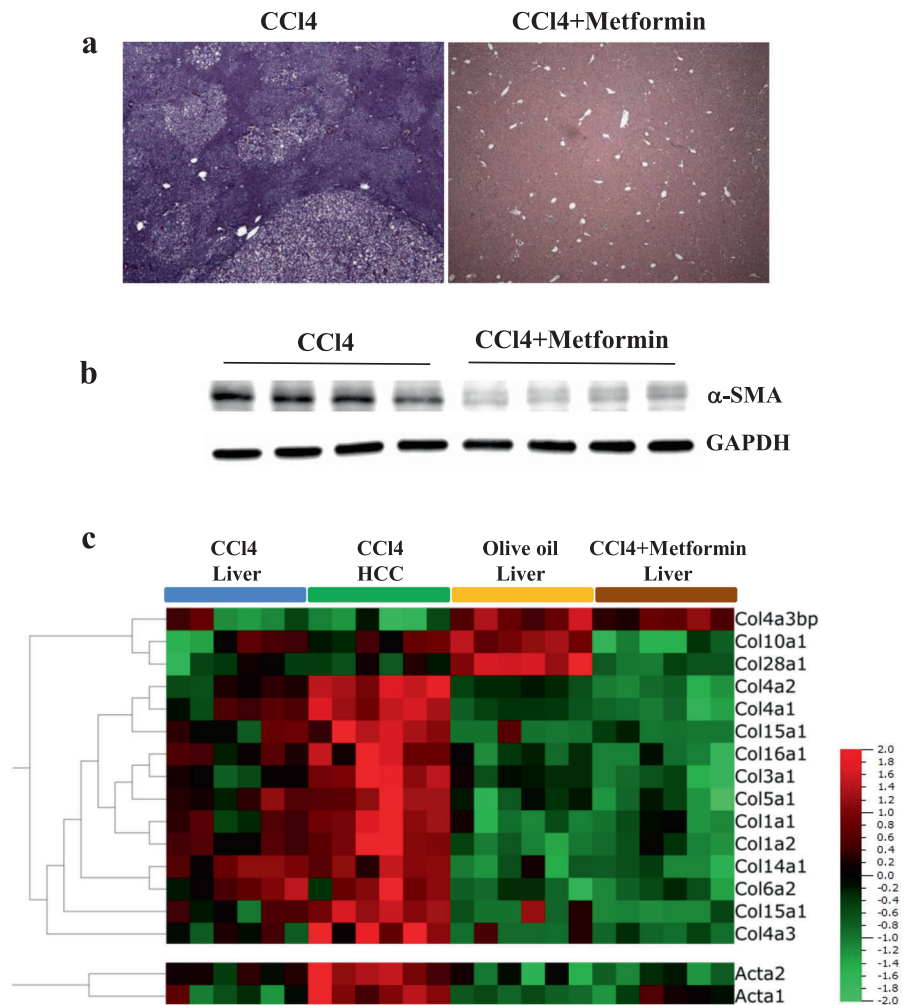
381 Metformin intervention at an early fibrosis stage dramati-  
 382 cally abrogated formation of tumour nodules (Fig. 5). His-  
 383 topathology of livers did not reveal any detectable in situ  
 384 nodules in metformin treated mice, whereas in CCl<sub>4</sub>-only

385 mice, abundant nodules varying from FNH-like to HCC  
 386 were noticed (Supplementary Table 1, Supplementary  
 387 Fig. 4).

388 Data on fibrosis and steatosis suggest that the change in  
 389 the microenvironment could prevent tumour appearance.  
 390 Additionally, GSEA performed on microarray data from  
 391 livers of untreated and metformin treated CCl<sub>4</sub> exposed  
 392 livers suggested direct effects on cancer-associated path-  
 393 ways. Hallmark gene sets enriched significantly for  
 394 mTORC1, KRAS and PI3K/AKT/mTOR signaling path-  
 395 ways (Supplementary Fig. 5), with metformin negatively  
 396 regulating these pathways. Confirming these indications, we  
 397 observed that metformin inhibited AKT phosphorylation in  
 398 liver tissue along with downstream key effectors S6 and 4E-  
 399 BP1 (Fig. 6). Albeit, metformin had no apparent effect on  
 400 total or phosphorylated status of mTOR (data not shown).  
 401 Since PI3K/AKT pathway is a key regulator of cell survival  
 402 [38], metformin-mediated inhibition of AKT resulted in a  
 403 higher level of apoptosis as demonstrated by the increased  
 404 cleavage of PARP (Fig. 6, Supplementary Fig. 6). None of  
 405 the proteins dysregulated through metformin treatment were  
 406 direct predicted miR-221 targets.

**Fig. 3** Metformin intervention reduces fibrosis in CCl<sub>4</sub>-challenged TG221 mice.

**a** Representative trichrome staining of FFPE livers at 24 weeks without and with metformin intervention. **b** Western blot analysis of  $\alpha$ -SMA protein in livers without and with metformin intervention. **c** Heat map for the expression of several collagen and  $\alpha$ -SMA genes (*Acta2*) in CCl<sub>4</sub> only livers, matched liver nodules, olive oil livers and CCl<sub>4</sub>+metformin treated livers. Intense red means the highest expression; intense green the lowest. Uncropped images of western blots are shown in Supplementary Fig. 6



407 Metabolism and bioactivation of CCl<sub>4</sub> in liver are pri- 425  
408 marily mediated by cytochrome P450 2E1 (CYP2E1) 426  
409 enzyme [39]. Thus, metformin could negatively regulate 427  
410 CYP2E1 expression and abrogate CCl<sub>4</sub>-mediated liver 428  
411 injury. However, we observed that gene expression of 429  
412 *Cyp2e1* in olive oil, CCl<sub>4</sub> and metformin+CCl<sub>4</sub> treated 430  
413 livers was not significantly dysregulated (Supplementary 431  
414 Table 2). Furthermore, GSEA was not significant for genes 432  
415 involved in regulation of transcription factor activity or 433  
416 several other cytochrome P450 enzymes involved in meta- 434  
417 bolism of xenobiotics or drugs were not enriched upon 435  
418 metformin intervention (Supplementary Table 3).

## 419 Discussion

420 By acting on aetiologic viral factors, like HBV or HCV, it 440  
421 has been possible to reduce the risk of virus-associated 441  
422 HCC. Either Hepatitis B immunization programs or anti- 442  
423 HCV direct-acting treatments have not only been beneficial 443  
424 to virus control, but also in reducing viral-associated HCC 444  
445

425 incidence [4, 40, 41]. However, chemoprevention strategies 426  
427 in non-viral related HCC remain a significant unmet medi- 428  
429 cal need. Although liver is the primary site of metformin 430  
431 function, to the best of our knowledge, hepatoprotective 432  
433 effects of early metformin intervention has been previously 434  
435 reported only once in a carcinogen-induced rat model of 436  
437 HCC [17]. The effect of metformin has also been investi- 438  
439 gated in patients with advanced HCC under sorafenib 440  
441 therapy. In this setting, metformin was not found to be 442  
443 effective, even possibly responsible for an increased tumour 444  
445 aggressiveness and a reduction of overall survival [42].

436 Several challenges are present in the preclinical devel- 437  
438 opment of secondary chemoprevention. Firstly, the diffi- 439  
440 culty of developing reliable mouse models capable of 441  
442 simulating the progressive evolution of liver disease from 443  
444 fibrosis to HCC has hitherto prevented testing experimen- 445  
446 tal prevention approaches. To this end, CCl<sub>4</sub> induced chronic 447  
448 liver injury in TG221 mouse model could reproduce all the 449  
450 mentioned phases and was crucial to perform prevention 451  
452 studies reported in this present study. Secondly, since 453  
454 pharmacological agents for early intervention are required 455

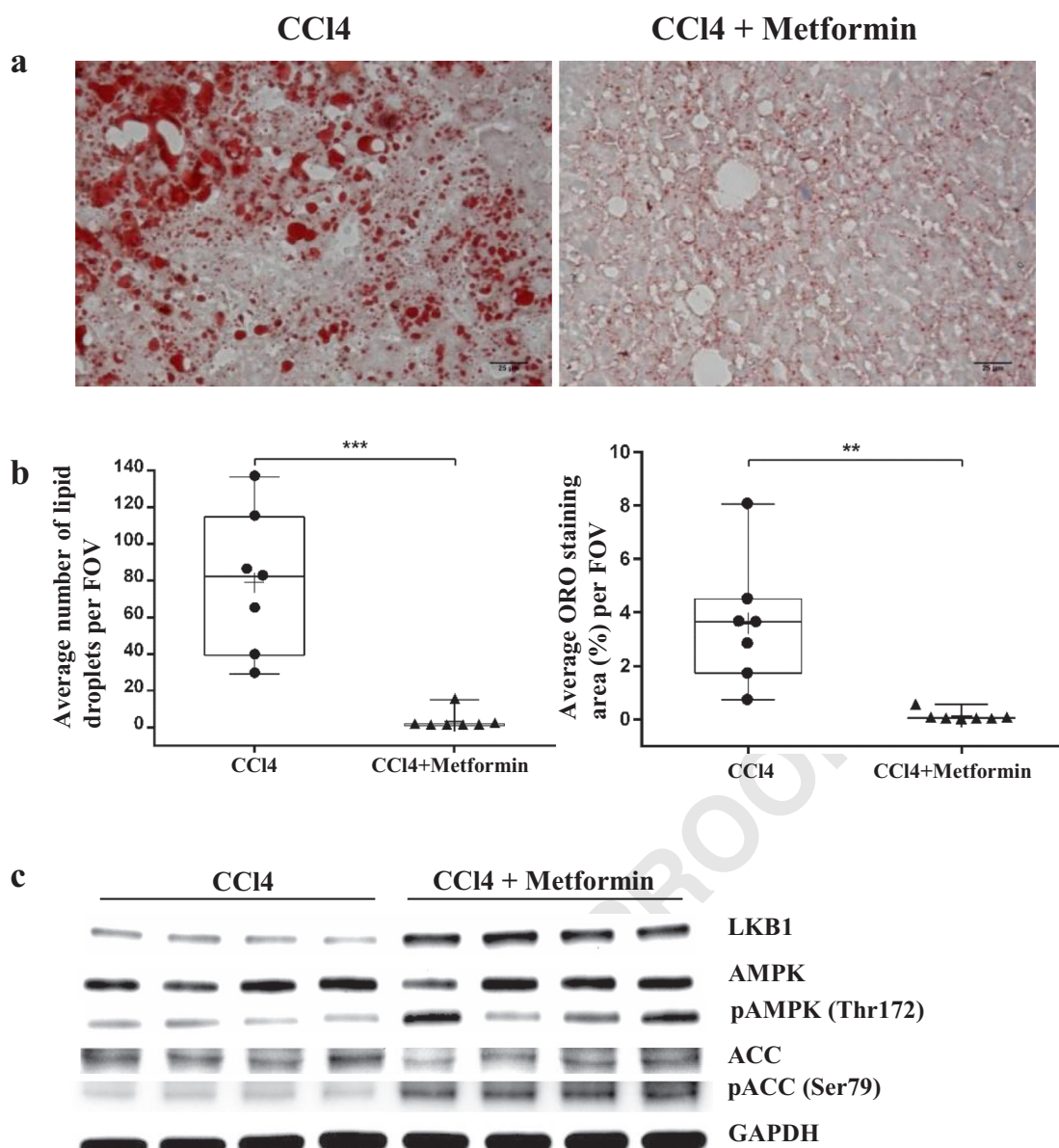


**Fig. 4** Metformin intervention reduces steatosis in CCl<sub>4</sub>-challenged TG221 mice. **a** Oil Red O (ORO) staining of sections from formalin fixed, OCT embedded and frozen livers at 24 weeks without and with metformin intervention. **b** Lipid droplets were morphometrically quantified after ORO staining for average number and percentage staining area per field of vision in CCl<sub>4</sub> and CCl<sub>4</sub>+metformin mice.

\*\*\* $P < 0.001$  \*\* $P < 0.01$ . Each data point represents a single mouse. **c** Western blot analyses show that metformin induces LKB1 mediated AMPK activation and leads to the downstream inhibitory phosphorylation of ACC at Ser-79, a rate-limiting step in fatty acid synthesis. Uncropped images of western blots are shown in Supplementary Fig. 6

446 to be administered for long periods of time, dictated by  
447 extended time to cancer progression, these agents should  
448 preferably be orally available and with minimal or no  
449 potential toxicity. Our results show that early intervention  
450 with metformin was effective in preventing HCC occur-  
451 rence in the TG221-CCl<sub>4</sub> mouse model. Oral administration  
452 of 300 mg/kg metformin, which approximately translates to  
453 standard 1500 mg/day taken by DM2 patients, abrogated  
454 formation of liver tumours in mice, thereby suggesting that  
455 secondary chemoprevention of HCC could be achieved in

456 patients with early signs of fibrosis at standard prescribed  
457 daily metformin dose.

458 Tumour initiation and progression is predominantly driven  
459 by conducive tissue environment that facilitates  
460 epithelial-mesenchymal transition (EMT), dysregulated  
461 metabolism and sustained proliferative signaling [43, 44].  
462 Cirrhosis microenvironment comprises all these features  
463 and represents the most important risk factor for HCC  
464 development.



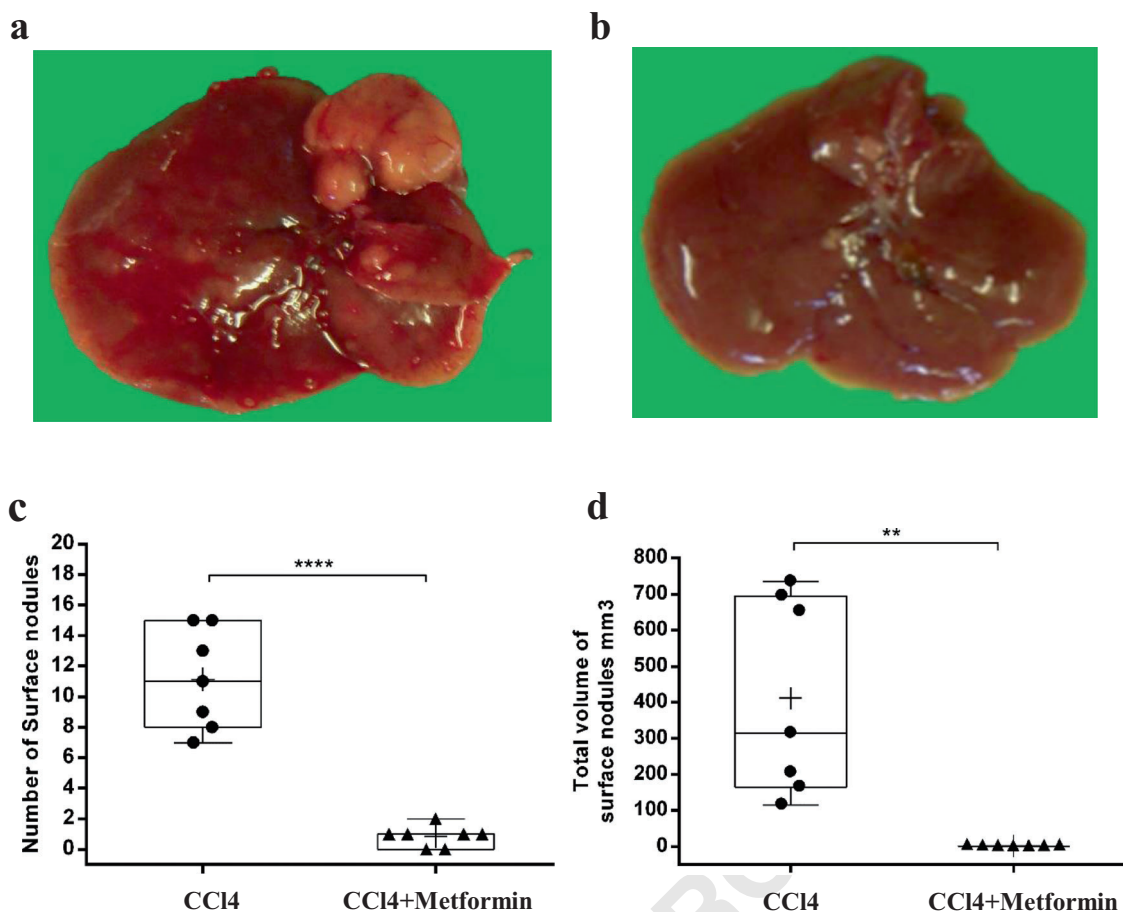


**Fig. 5** Metformin intervention prevents the appearance of tumour nodules in CCl<sub>4</sub>-challenged TG221 mice. **a** Representative liver from a CCl<sub>4</sub>-challenged mouse control. **b** Representative liver from a mouse treated with CCl<sub>4</sub> and metformin. **c, d** Surface nodules: number and

volume in CCl<sub>4</sub> mice in comparison with mice that received CCl<sub>4</sub>+metformin. The latter did not develop any tumour nodules. \*\*\*\**P* < 0.0001 \*\**P* < 0.01 Each data point represents a single mouse

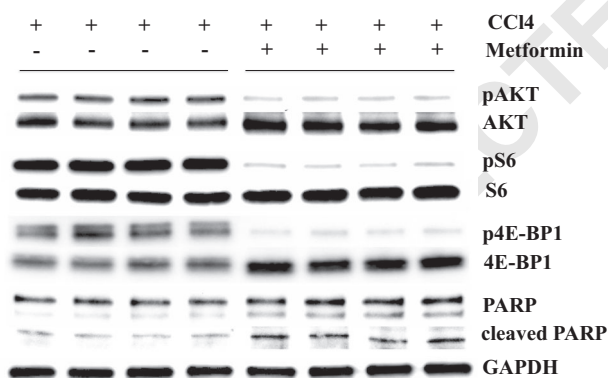


**Fig. 6** Metformin intervention modulates the AKT pathway and apoptosis in liver tissue of CCl<sub>4</sub>-challenged TG221 mice. Western blot analyses of AKT, S6, 4E-BP1 and PARP in liver tissue from CCl<sub>4</sub> and metformin treated mice. GAPDH was used an internal loading control. Uncropped images of western blots are shown in Supplementary Fig. 6

collagens and contribute to EMT [45, 46]. Here, we show that metformin inhibited the activation of HSCs as evidenced by reduced  $\alpha$ -SMA and collagen (*Col1a1*, *Col4a1*, *Col4a2*) expression levels, thereby reducing liver fibrosis. Additionally, GSEA revealed negative regulation of set of hallmark EMT genes (NES = -2.40, FDR = 0.002) by metformin, which supports the inhibition of EMT process. Furthermore, metformin intervention resulted in LKB1 mediated AMPK activation, which is considered a key regulator of metabolic and energy homeostasis and downstream inhibition of ACC [37, 47, 48]. This resulted in significant reduction of microvesicular steatosis in livers. Earlier *in vivo* studies reported that loss of lipid droplets in HSCs in chronically injured livers might suppress tumourigenesis [49].

GSEA provided additional valuable insights into effects of metformin on cellular proliferation/survival signalling pathways, most importantly PI3K/AKT/mTOR pathway. Although we did not detect any effect of metformin on mTOR, suppression of AKT and its downstream effectors

Our results indicate that metformin acts primarily to normalize fibrotic and steatotic microenvironment typical of cirrhosis. In fibrotic liver, activated HSCs produce various

explains the pro-apoptotic liver environment which negatively influenced liver tumourigenesis. Indeed, liver injury induced by CC14 resulted in liver enlargement and fibrosis. However, the apoptotic effect promoted by metformin suggests that cell death could possibly antagonize liver proliferative reaction to chronic injury. Previous studies in carcinogen-induced and spontaneous mouse models have reported that targeting AKT or metformin mediated AKT suppression, has been beneficial in preventing lung tumours [50–52].

Our findings carry the promise for a medical application. While a number of clinical studies established that metformin reduces the risk of developing HCC in type 2 DM patients [53] (Supplementary Table 4), our results indicate that its prophylactic activity can be expanded to patients with liver fibrosis at risk of developing cirrhosis and HCC, regardless of concomitant type 2 DM. The translational value is high, as it involves a potentially large number of individuals. According to epidemiological studies in US and Europe, prevalence of cirrhosis was estimated at about 0.3% of population [54–56], probably an underestimate considering that early stages of cirrhosis are asymptomatic. In addition to reducing the risk of HCC occurrence, our results establish that the use of metformin in early stages of liver fibrosis can effectively ameliorate the underlying liver disease despite continued exposure to aetiological risk factors, suggesting that this approach could equip clinicians for a better management of chronic liver disease as well as prevention of HCC.

In conclusion, metformin intervention resulted in improved liver function, reduced fibrosis, decreased dependence on lipids as primary source of energy and most importantly abrogated the appearance of liver tumours. Low cost, long-term tolerability and safety of metformin provide a strong rationale for chemoprevention in liver fibrosis patients who are at high risk of developing liver cancer.

**Acknowledgements** This work was supported by the Italian Association for Cancer Research (AIRG IG-15615, AIRC IG-20055) to Massimo Negrini, PhD.

## Compliance with ethical standards

**Conflict of interest** The authors declare that they have no conflict of interest.

**Publisher's note:** Springer Nature remains neutral with regard to jurisdictional claims in published maps and institutional affiliations.

## References

1. Bray F, Ferlay J, Soerjomataram I, Siegel RL, Torre LA, Jemal A. Global cancer statistics 2018: GLOBOCAN estimates of incidence and mortality worldwide for 36 cancers in 185 countries. *CA: a cancer J Clin.* 2018;68:394–424.

2. El-Serag HB. Hepatocellular carcinoma. *New Engl J Med.* 2011;365:1118–27. 537

3. Llovet JM, Zucman-Rossi J, Pikarsky E, Sangro B, Schwartz M, Sherman M, et al. Hepatocellular carcinoma. *Nat Rev Dis Prim.* 2016;2:16018. 538

4. Ioannou GN, Green PK, Berry K. HCV eradication induced by direct-acting antiviral agents reduces the risk of hepatocellular carcinoma. *J Hepatol.* 2017. 539

5. Nordenstedt H, White DL, El-Serag HB. The changing pattern of epidemiology in hepatocellular carcinoma. *Dig Liver Dis.* 2010;42:S206–14. 540

6. Global Burden of Disease Liver Cancer C, Akinyemiju T, Abera S, Ahmed M, Alam N, Alemayohu MA, et al. The burden of primary liver cancer and underlying etiologies from 1990 to 2015 at the global, regional, and national level: results from the global burden of disease study 2015. *JAMA Oncol.* 2017;3:1683–91. 541

7. Fukumura D, Incio J, Shankaraiah R, Jain RK. Obesity and cancer: an angiogenic and inflammatory link. *Microcirculation.* 2016;23:191–206. 542

8. Yoon K-H, Lee J-H, Kim J-W, Cho JH, Choi Y-H, Ko S-H, et al. Epidemic obesity and type 2 diabetes in Asia. *Lancet.* 2006;368:1681–8. 543

9. Bo S, Ciccone G, Rosato R, Villosio P, Appendino G, Ghigo E, et al. Cancer mortality reduction and metformin: a retrospective cohort study in type 2 diabetic patients. *Diabetes, Obes Metab.* 2012;14:23–29. 544

10. Lee JH, Kim TI, Jeon SM, Hong SP, Cheon JH, Kim WH. The effects of metformin on the survival of colorectal cancer patients with diabetes mellitus. *Int J Cancer.* 2012;131:752–9. 545

11. Lee MS, Hsu CC, Wahlqvist ML, Tsai HN, Chang YH, Huang YC. Type 2 diabetes increases and metformin reduces total, colorectal, liver and pancreatic cancer incidences in Taiwanese: a representative population prospective cohort study of 800,000 individuals. *BMC Cancer.* 2011;11:20. 546

12. Nkontchou G, Cosson E, Aout M, Mahmoudi A, Bourcier V, Charif I, et al. Impact of metformin on the prognosis of cirrhosis induced by viral hepatitis C in diabetic patients. *J Clin Endocrinol Metab.* 2011;96:2601–8. 547

13. Dasgupta B, Chhipa RR. Evolving lessons on the complex role of AMPK in normal physiology and cancer. *Trends Pharmacol Sci.* 2016;37:192–206. 548

14. Yang X, Liu Y, Li M, Wu H, Wang Y, You Y, et al. Predictive and preventive significance of AMPK activation on hepatocarcinogenesis in patients with liver cirrhosis. *Cell Death Dis.* 2018;9:264. 549

15. Incio J, Suboj P, Chin SM, Vardam-Kaur T, Liu H, Hato T, et al. Metformin reduces desmoplasia in pancreatic cancer by reprogramming stellate cells and tumor-associated macrophages. *PLoS ONE.* 2015;10:e0141392. 550

16. Qian W, Li J, Chen K, Jiang Z, Cheng L, Zhou C, et al. Metformin suppresses tumor angiogenesis and enhances the chemosensitivity of gemcitabine in a genetically engineered mouse model of pancreatic cancer. *Life Sci.* 2018;208:253–61. 551

17. DePeralta DK, Wei L, Ghoshal S, Schmidt B, Lauwers GY, Lanuti M, et al. Metformin prevents hepatocellular carcinoma development by suppressing hepatic progenitor cell activation in a rat model of cirrhosis. *Cancer.* 2016;122:1216–27. 552

18. Kim JH, Lee KJ, Seo Y, Kwon JH, Yoon JP, Kang JY, et al. Effects of metformin on colorectal cancer stem cells depend on alterations in glutamine metabolism. *Sci Rep.* 2018;8:409. 553

19. Casadei Gardini A, Marisi G, Scarpi E, Scartozzi M, Faloppi L, Silvestris N, et al. Effects of metformin on clinical outcome in diabetic patients with advanced HCC receiving sorafenib. *Expert Opin Pharmacother.* 2015;16:2719–25. 554

20. Reagan-Shaw S, Nihal M, Ahmad N. Dose translation from animal to human studies revisited. *FASEB J.* 2008;22:659–61. 555

- 603 21. Kodack DP, Askoxylakis V, Ferraro GB, Sheng Q, Badeaux M, Goel S, et al. The brain microenvironment mediates resistance in luminal breast cancer to PI3K inhibition through HER3 activation. *Science translational medicine* 2017; 9.
- 604  
605  
Q146
- 607 22. Deutsch MJ, Schriever SC, Roscher AA, Ensenauer R. Digital image analysis approach for lipid droplet size quantitation of Oil Red O-stained cultured cells. *Anal Biochem.* 2014;445:87–89.
- 608  
609
- 610 23. Donadon V, Balbi M, Ghersetti M, Grazioli S, Perciaccante A, Valentina GD, et al. Antidiabetic therapy and increased risk of hepatocellular carcinoma in chronic liver disease. *World J Gastroenterol.* 2009;15:2506.
- 611  
612  
613
- 614 24. Mootha VK, Lindgren CM, Eriksson KF, Subramanian A, Sihag S, Lehar J, et al. PGC-1 $\alpha$ -responsive genes involved in oxidative phosphorylation are coordinately downregulated in human diabetes. *Nat Genet.* 2003;34:267–73.
- 615  
616  
617
- 618 25. Subramanian A, Tamayo P, Mootha VK, Mukherjee S, Ebert BL, Gillette MA, et al. Gene set enrichment analysis: a knowledge-based approach for interpreting genome-wide expression profiles. *Proc Natl Acad Sci USA.* 2005;102:15545–50.
- 619  
620  
621
- 622 26. Liu W, Wang X. Prediction of functional microRNA targets by integrative modeling of microRNA binding and target expression data. *Genome Biol.* 2019;20:18.
- 623  
624
- 625 27. Faul F, Erdfelder E, Buchner A, Lang AG. Statistical power analyses using G\*Power 3.1: tests for correlation and regression analyses. *Behav Res Methods.* 2009;41:1149–60.
- 626  
627
- 628 28. Callegari E, Elamin BK, Giannone F, Milazzo M, Altavilla G, Fornari F, et al. Liver tumorigenicity promoted by microRNA-221 in a mouse transgenic model. *Hepatology.* 2012;56:1025–33.
- 629  
630
- 631 29. European Association For The Study Of The L, European Organisation For R, Treatment Of C. EASL-EORTC clinical practice guidelines: management of hepatocellular carcinoma. *J Hepatol.* 2012;56:908–43.
- 632  
633  
634
- 635 30. Muir AJ. Understanding the complexities of cirrhosis. *Clin Ther.* 2015;37:1822–36.
- 636  
637
- 638 31. Murff HJ, Roumie CL, Greevy RA, Hackstadt AJ, McGowan LED, Hung AM, et al. Metformin use and incidence cancer risk: evidence for a selective protective effect against liver cancer. *Cancer Causes Control.* 2018;29:823–32.
- 639  
640
- 641 32. Gluchowski NL, Becuwe M, Walther TC, Farese RV Jr. Lipid droplets and liver disease: from basic biology to clinical implications. *Nat Rev Gastroenterol Hepatol.* 2017;14:343–55.
- 642  
643
- 644 33. Tandra S, Yeh MM, Brunt EM, Vuppalanchi R, Cummings OW, Unalp-Arida A, et al. Presence and significance of microvesicular steatosis in nonalcoholic fatty liver disease. *J Hepatol.* 2011;55:654–9.
- 645  
646  
647
- 648 34. Kim J, Yang G, Kim Y, Kim J, Ha J. AMPK activators: mechanisms of action and physiological activities. *Exp Mol Med.* 2016;48:e224.
- 649  
650
- 651 35. Hardie DG. AMP-activated protein kinase: an energy sensor that regulates all aspects of cell function. *Genes Dev.* 2011;25:1895–908.
- 652  
653
- 654 36. Hassan MM, Curley SA, Li D, Kaseb A, Davila M, Abdalla EK, et al. Association of diabetes duration and diabetes treatment with the risk of hepatocellular carcinoma. *Cancer.* 2010;116:1938–46.
- 655  
656  
657
- 658 37. Fullerton MD, Galic S, Marcinko K, Sikkema S, Pulinilkunnil T, Chen ZP, et al. Single phosphorylation sites in Acc1 and Acc2 regulate lipid homeostasis and the insulin-sensitizing effects of metformin. *Nat Med.* 2013;19:1649–54.
- 659  
660
- 661 38. Vivanco I, Sawyers CL. The phosphatidylinositol 3-Kinase AKT pathway in human cancer. *Nat Rev Cancer.* 2002;2:489–501.
- 662
- 663 39. Wong FW, Chan WY, Lee SS. Resistance to carbon tetrachloride-induced hepatotoxicity in mice which lack CYP2E1 expression. *Toxicol Appl Pharmacol.* 1998;153:109–18.
- 664  
665
- 666 40. Kao J-H, Chen D-S. Global control of hepatitis B virus infection. *Lancet Infect Dis.* 2002;2:395–403.
- 667
- 668 41. Kasmari AJ, Welch A, Liu G, Leslie D, McGarrity T, Riley T. Independent of cirrhosis, hepatocellular carcinoma risk is increased with diabetes and metabolic syndrome. *Am J Med.* 2017;130:746 e741–746 e747.
- 669  
670  
671
- 672 42. Casadei Gardini A, Faloppi L, De Matteis S, Foschi FG, Silvestris N, Tovoli F, et al. Metformin and insulin impact on clinical outcome in patients with advanced hepatocellular carcinoma receiving sorafenib: Validation study and biological rationale. *Eur J Cancer.* 2017;86:106–14.
- 673  
674  
675  
676
- 677 43. Hanahan D, Weinberg RA. Hallmarks of cancer: the next generation. *Cell.* 2011;144:646–74.
- 678
- 679 44. Tennant DA, Duran RV, Boulahbel H, Gottlieb E. Metabolic transformation in cancer. *Carcinogenesis.* 2009;30:1269–80.
- 680
- 681 45. Kalluri R, Weinberg RA. The basics of epithelial-mesenchymal transition. *J Clin Invest.* 2009;119:1420–8.
- 682
- 683 46. Tsuchida T, Friedman SL. Mechanisms of hepatic stellate cell activation. *Nat Rev Gastroenterol Hepatol.* 2017;14:397–411.
- 684
- 685 47. Chaube B, Bhat MK. AMPK, a key regulator of metabolic/energy homeostasis and mitochondrial biogenesis in cancer cells. *Cell Death Dis.* 2016;7:e2044.
- 686  
687
- 688 48. Chen HP, Shieh JJ, Chang CC, Chen TT, Lin JT, Wu MS, et al. Metformin decreases hepatocellular carcinoma risk in a dose-dependent manner: population-based and in vitro studies. *Gut.* 2013;62:606–15.
- 689  
690  
691
- 692 49. Kluwe J, Wongsiriroj N, Troeger JS, Gwak GY, Dapito DH, Pradere JP, et al. Absence of hepatic stellate cell retinoid lipid droplets does not enhance hepatic fibrosis but decreases hepatic carcinogenesis. *Gut.* 2011;60:1260–8.
- 693  
694  
695
- 696 50. Hollander MC, Maier CR, Hobbs EA, Ashmore AR, Linnoila RI, Dennis PA. Akt1 deletion prevents lung tumorigenesis by mutant K-ras. *Oncogene.* 2011;30:1812–21.
- 697  
698
- 699 51. Linnerth-Petrik NM, Santry LA, Petrik JJ, Wootton SK. Opposing functions of Akt isoforms in lung tumor initiation and progression. *PLoS ONE.* 2014;9:e94595.
- 700  
701
- 702 52. Memmott RM, Mercado JR, Maier CR, Kawabata S, Fox SD, Dennis PA. Metformin prevents tobacco carcinogen-induced lung tumorigenesis. *Cancer Prev Res.* 2010;3:1066–76.
- 703  
704
- 705 53. Singh S, Singh PP, Singh AG, Murad MH, Sanchez W. Anti-diabetic medications and the risk of hepatocellular cancer: a systematic review and meta-analysis. *Am J Gastroenterol.* 2013;108:881–91. quiz 892
- 706  
707  
708
- 709 54. Blachier M, Leleu H, Peck-Radosavljevic M, Valla DC, Roudot-Thoraval F. The burden of liver disease in Europe: a review of available epidemiological data. *J Hepatol.* 2013;58:593–608.
- 710  
711
- 712 55. Scaglione S, Kliethermes S, Cao G, Shoham D, Durazo R, Luke A, et al. The Epidemiology of cirrhosis in the United States: a population-based Study. *J Clin Gastroenterol.* 2015;49:690–6.
- 713  
714
- 715 56. Schulte L, Scheiner B, Voigtlander T, Koch S, Schweitzer N, Marhenke S, et al. Treatment with metformin is associated with a prolonged survival in patients with hepatocellular carcinoma. *Liver Int.* 2019;39:714–26.
- 716  
717  
718

Journal : 41388

Article : 942

**SPRINGER NATURE**

## Author Query Form

**Please ensure you fill out your response to the queries raised below and return this form along with your corrections**

Dear Author

During the process of typesetting your article, the following queries have arisen. Please check your typeset proof carefully against the queries listed below and mark the necessary changes either directly on the proof/online grid or in the 'Author's response' area provided below

Queries	Details Required	Author's Response
AQ1	Since the references were not cited in numerical order, they have been renumbered in the order of appearance. Please check.	
AQ2	Please check your article carefully, coordinate with any co-authors and enter all final edits clearly in the eproof, remembering to save frequently. Once corrections are submitted, we cannot routinely make further changes to the article.	
AQ3	Note that the eproof should be amended in only one browser window at any one time; otherwise changes will be overwritten.	
AQ4	Author surnames have been highlighted. Please check these carefully and adjust if the first name or surname is marked up incorrectly. Note that changes here will affect indexing of your article in public repositories such as PubMed. Also, carefully check the spelling and numbering of all author names and affiliations, and the corresponding email address(es).	
AQ5	Please note that after the paper has been formally accepted you can only provide amended Supplementary Information files for critical changes to the scientific content, not for style. You should clearly explain what changes have been made if you do resupply any such files.	
AQ6	Should you wish to order offprints, please click on <a href="http://www.nature.com/aj/forms/onc_offprint_2017.pdf">www.nature.com/aj/forms/onc_offprint_2017.pdf</a> to download and complete the offprint form and upload the completed form along with the article.	
AQ7	Original reference 12 was not originally cited in text. Please confirm that the citation of this reference after the sentence 'as described previously' is ok.	
AQ8	Original reference 41 was not originally cited in text. Please confirm that the citation of this reference after the sentence 'deterioration of fibrotic disease' is ok.	
AQ9	Original reference 22 was not originally cited in text. Please confirm that the citation of this reference after the sentence 'metabolism and energy homeostasis' is ok.	
AQ10	Original reference 28 was not originally cited in text. Please confirm that the citation of this reference after the sentence 'viral-associated HCC incidence' is ok.	
AQ11	Original reference 8 was not originally cited in text. Please confirm that the citation of this reference after the sentence 'downstream inhibition of ACC' is ok.	
AQ12	Original reference 47 was not originally cited in text. Please confirm that the citation of this reference after the sentence 'about 0.3% of population' is ok.	
AQ13	Please provide the page range or volume number for reference 4.	
AQ14	Please provide the page range for reference 21.	